Ultrathin Coating of Bioactive Microcapsules Enhances Phenotype of Encapsulated Pluripotent Stem Cells

Daheui Choi[a], Kihak Gwon[a], Hye Jin Hong[a], Harihara Baskaran[b], Olalla Calvo-Lozano[c], Alan M. Gonzalez-Suarez[a], Kyungtae Park[d], Jose M. de Hoyos-Vega[a], Laura M. Lechuga[c], Jinkee Hong[d], Gulnaz Stybayeva[a] and Alexander Revzin[a,*]

[a] Department of Physiology and Biomedical Engineering, Mayo Clinic, Rochester, MN, 55902, USA

[b] Department of Chemical and Biomolecular Engineering, Case Western Reserve University, Cleveland, OH, 44106, USA

[c] Nanobiosensors and Bioanalytical Applications Group (NanoB2A), Catalan Institute of Nanoscience and Nanotechnology (ICN2), CSIC, CIBERBBN and BIST, Barcelona 08193, Spain

[d] Department of Chemical and Biomolecular Engineering, Yonsei University, Seoul 03722, Republic of Korea

* Correspondence: revzin.alexander@mayo.edu

ABSTRACT

Human pluripotent stem cells (hPSCs) may be differentiated into any adult cell type and therefore hold incredible promise for cell therapeutics and disease modeling. There is increasing interest in three dimensional (3D) hPSC culture formats because it reflects growth nature with better understanding of cell-cell niche. Our team has recently described bioactive heparin-containing core-shell microcapsules that promote rapid aggregation of stem cells into spheroids and may also be loaded with growth factors for local and sustained delivery to the encapsulated cells. In this study, we explored the possibility of further modulating bioactivity of microcapsules through the use of ultrathin coating comprised of tannic acid (TA). We used ellipsometry and atomic force microscope (AFM) to determine that TA coating was 6.5 nm and 4.108 nm in thickness and roughness when deposited onto a model substrate. TA-coated microcapsules had a 4-fold lower permeability compared to control microcapsules. Furthermore, the presence of the TA coating was observed to increase the amount of basic fibroblast growth factor (bFGF) incorporation up to 189% and extend its release from 5 days to 10 days. Most significantly, TA-microcapsules loaded with bFGF induced higher levels of pluripotency expression compared to uncoated microcapsules containing bFGF. Engineered microcapsules described here represent a new stem cell culture approach that enables 3D cultivation and relies on local delivery of inductive cues.

Keywords: Microfluidics, Heparin-based microcapsules, Tannic acid, Nanofilm, Controlled growth factor release, 3D stem cell cultures

1. INTRODUCTION

Human pluripotent stem cells (hESCs) are capable of unlimited proliferation and may be differentiated into any adult cell type.[1, 2] Because of these properties, hPSCs hold incredible potential as a source of adult cells for cellular therapies, tissue engineering and disease modeling.[3-5] Increasingly, stem cell biology community has recognized both biological (e.g. improved differentiation outcomes) and practical benefits (e.g. scale-up) of cultivating hPSCs in a 3D format.[6-9] 3D culture formats recently reported in the literature include hanging drop,[10, 11] scaffold-based 3D culture,[12] as well as spheroid cultures under stirring or rocking conditions. [13-16] Despite these published reports, there remains a need for efficient and cost-effective differentiation protocols.

Microcapsules represent an interesting stem cell culture format that offers a number of benefits.[17-20] Because the hydrogel-based microcapsules provide semipermeable and biocompatible 3D environments to cells, the tissue-like environments and retention of oxygen or nutrients levels with blockage of external stresses could be realized in capsules.[21, 22] For example, inspired by the natural proliferation and differentiation of blastomeres in hydrogel shell-like structure, the core-shell hydrogel microcapsules that encapsulate iPSC clusters were produced by microfluidic technique.[23] 3D development of iPSCs in microcapsules showed better pluripotent expression and differentiation potential compared to 2D culture. Another group developed iPSC-encapsulated photocrosslinkable PEG-fibrinogen microspheres for cardiac differentiation, showing the possibility to large-scale production of cardiomyocytes with higher reproducibility.[24] Our team has previously demonstrated that microcapsules with polyethylene glycol (PEG) hydrogel shell and aqueous core may be used to 1) promote aggregation of encapsulated stem cells into spheroids and 2) protect

encapsulated spheroids against mechanical agitation in a stirred bioreactor.[25] Most recently we described bioactive heparin-containing core-shell microcapsules that could be loaded with growth factors for local and sustained delivery of inductive cues to the encapsulated hPSC spheroids.[26]

In the present study, we wanted to further modulate physicochemical and biological properties of our microcapsules through the use of an ultrathin coating. There have been a number of reports describing ultrathin coating approaches for stem cell cultivation and differentiation.[27-31] Since the last decade, multilayer films using polyelectrolytes such as heparin or chondroitin sulfate have been prepared to control the loading and release of growth factors for proliferation and differentiation of stem cells.[27] As a more advanced method for enhancing stem cells functions, the direct multilayer nanofilm coating on iPSCs using vitronectin or fibronectin to mimic ECM conditions was investigated.[30, 31] Point out that to the best of our knowledge, there is no report where ultrathin coating is applied to a microcapsule that contains stem cells. We chose to employ tannic acid (TA), a polyphenol derivative comprised of gallic acid linked to a glucose core, because of its biocompatibility and ease of deposition.[32, 33] The multiple phenolic groups in TA alter charge density depending in the pH condition.[34] Also, TA can be stably crosslinked through interactions with several multi-valent metal ions including Fe^{3+}, Co^{2+} and Cu^{2+} under neutral pH (see Scheme 1).[35] We chose to work with Fe ions in this study because of its highest linkability and biocompatibility among the other metal ions.[36] Presence of phenyl groups in the TA structure promotes hydrogen bonding and hydrophobic interactions with proteins.[37, 38] We hypothesized that an ultrathin coating may be used to further modulate bioactivity of our heparin-containing microcapsules. In this study, we describe overcoating of microcapsules with an ultrathin film of TA. We first characterized film assembly, thickness and surface

morphology, on a model planer substrate (silicon) and then proceeded to coat microcapsules. Subsequently, we characterized the effects of TA overcoat on permeability and growth factor loading/release properties of heparin-based microcapsules. Finally, we demonstrated that the presence of TA overcoat improved pluripotency expression of encapsulated hPSC spheroids.

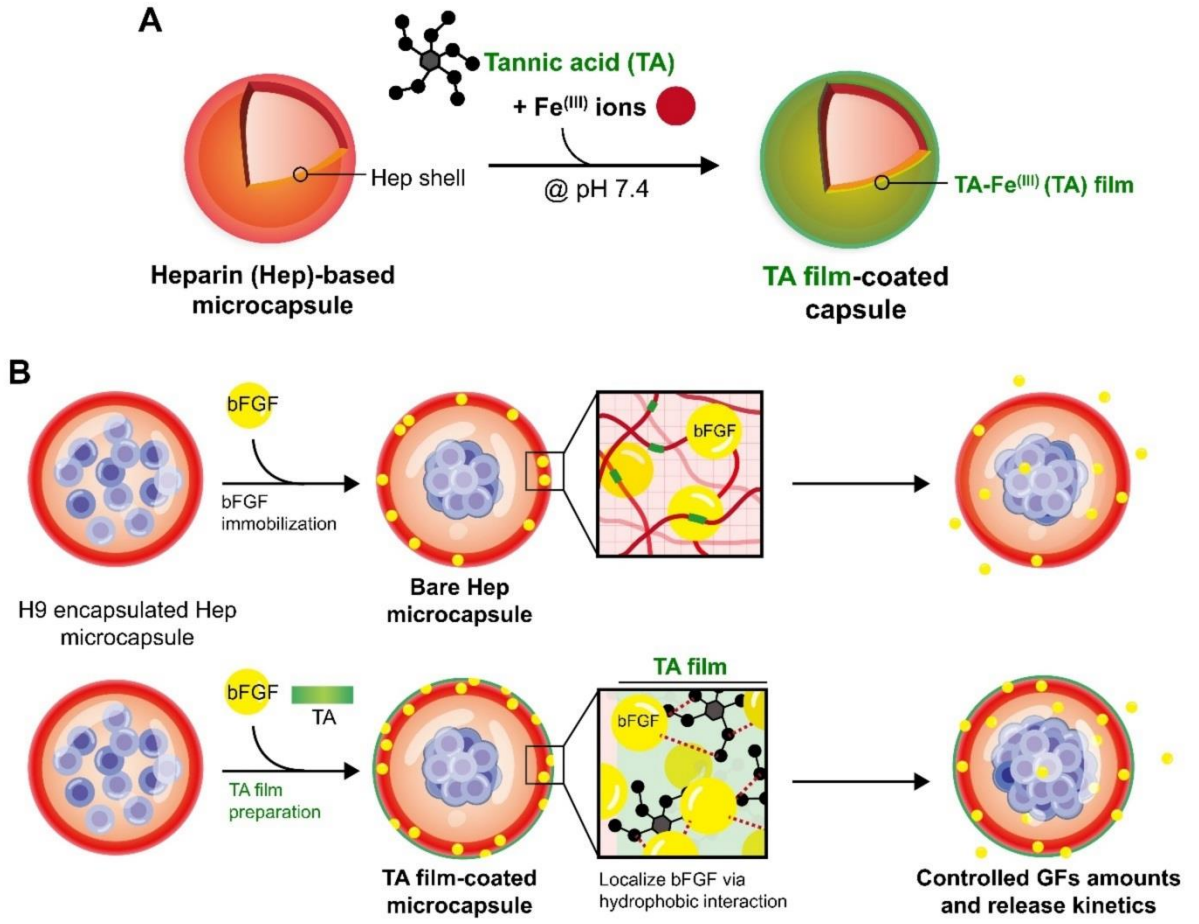

Scheme 1. Schematic illustrating ultrathin coating of stem cell-containing microcapsules. (**A**) TA molecules were cross-linked with Fe^{3+} ions to form a film atop and within a hydrogel microcapsule. (**B**) Microcapsules were comprised of a Hep-PEG hydrogel shell and an aqueous core and carried pluripotent stem cells. Properties of bare and coated microcapsules were compared with respect to loading/release of bFGF (an inductive cue) as well as pluripotency maintenance of the encapsulated stem cells.

2. MATERIALS AND METHODS

2.1. Materials

Sodium heparin was purchased from Smithfield Bioscience (Cincinnati, OH, USA). Methacrylic anhydride (MA), absolute ethanol, 1-Ethyl-3-(3-dimethylaminopropyl) carbodiimide (EDC), cysteamine, dithiothreitol (DTT), 35kDa PEG, triethanolamine (TEA), mineral oil, Span-80, iron (III) chloride hexahydrate ($FeCl_3 6H_2O$), TA, deferiprone (DFP), fluorescein isothiocyanate (FITC) and bovine serum albumin (BSA) were from Sigma-Aldrich (St. Louis, MO, USA). 3.5 kDa Mw cut-off (MWCO) dialysis bag was purchased from Spectrum Laboratories (Rancho Dominguez, CA, USA). 1-Hydroxybenzotriazole hydrate (HOBT) was from AnaSpec Inc (Fremont, CA, USA). 10 kDa 4-arm PEG-maleimide (PEG4MAL) was purchased from Laysan Inc (Arab, AL, USA). We followed previously published protocols to synthesize heparin-methacrylate (Hep-MA)[26] and heparin-thiol (Hep-SH).[39, 40]

Passage 3 Mouse embryonic fibroblast (MEFs) (EmbryoMaxR PMEF P3, Strain CF-1, Untreated) was purchased from MilliporeSigma (Burlington, MA, USA). Dulbecco's Modified Eagle Medium (DMEM), ES-FBS, Penicillin-streptomycin (P/S), DMEM/F12, KnockOut Serum Replacer (KOSR), Non-essential amino acids (NEAA), GlutaMAX, 2-mercaptoethanol and TrypLE™ Express were purchased from Thermo Fisher Scientific (Waltham, MA, USA). AgreeWell 400, Optiprep densifier and mTeSR medium were from STEMCELL Technologies (Vancouver, Canada). Live/Dead staining kit and donkey anti-mouse IgG secondary antibody-Alexa Fluor 546 were obtained from Invitrogen (Waltham, MA, USA). Anti-SOX2 antibody, bFGF, and ELISA kit for bFGF were purchased from R&D

systems (Minneapolis, MN, USA). DAPI was from Vectorlab (San Francisco, CA, USA).100 μm cell strainer was from Cardinal Health (Dublin, OH, USA). RNA extraction kit (RNeasy kit) was obtained from Qiagen (Valencia, CA, USA). OCT compound was purchased from Fisher Healthcare (Waltham, MA, USA).

2.2. Maintaining and expanding pluripotent stem cells

We used human embryonic stem cell (hESC) line H9 in this study. H9 cells were maintained on irradiated MEF feeder layer. P3 MEFs were cultured and expanded for two more passages (P5) in a media based on DMEM with 10% ES-FBS, 1% P/S, and 2 mM GlutaMAX. The cells at passage 5 were trypsinized, collected in a 15 mL conical tube, then irradiated at 20 Gy to mitotically inactivate them as feeder cells. The irradiated MEFs were cryopreserved at a concentration of 2×10^6 cells/vial for later use.

MEFs were seeded in a 6 well-plate with a concentration of 3×10^5 cells/well and cultured for 24 h. Afterwards, MEF media was removed and H9 cells were seeded at a concentration of 2×10^4 cells/well. Pluripotency media (referred to as H9 media in the paper) was composed of DMEM/F12, 20% KOSR, 1× NEAA, 2 mM GlutaMAX, 0.1 mM 2-mercaptoethanol, and 100 ng/mL bFGF. Media (2 mL per well) was changed daily over the course of 5 days. Unencapsulated H9 spheroids were used as one of the controls for our study. These spheroids were created by seeding of H9 cells into a commercial 3D culture plate (AggreWell). We previously determined that this cell concentration resulted in seeding density of ~200 cells per well and produced spheroids that were comparable in dimensions (150 μm diameter) to those observed inside microcapsules. H9 media (see above for composition) was used for cultivation of spheroids in AggreWell plates. Media was changed

every other day.

2.3. Fabrication of microfluidic devices for stem cell encapsulation

We have previously described a microfluidic encapsulation system consisting of a filtration device located upstream of a flow-focusing capsule fabrication device.[26] Detailed protocols for fabricating and operating this encapsulation system have been reported elsewhere.[26, 41] Briefly, co-axial flow-focusing device for cell encapsulation was fabricated using polydimethylsiloxane (PDMS) soft lithography. A device consisted of a total of four PDMS layers that were arranged into mirrored halves, each half with structures of three different heights. The mirrored PDMS slabs were treated with oxygen plasma and bonded to create a non-planar (3D) co-axial flow focusing device. This device had channels of three heights: (1) 120 μm for the aqueous core channel, (2) 200 μm for aqueous shell channels, and (3) 300 μm for shielding oil, crosslinker oil, and capsule collection channels. The filtration microfluidic device consisted of a single 50 μm tall chamber populated with 200 μm triangle posts. The spacing between the posts varied from 400 μm at the inlet to 30 at the outlet.[16] This device was designed to trap cell aggregates and to ensure that single cells but not cell clusters entered the capsule fabrication device.

2.4. Operation of the microfluidic cell encapsulation system

Fabrication of core-shell microcapsules proceeded as follows. The coaxial flow-focusing microfluidic device was loaded with 4 different solutions: (1) core solution with 8% (w/v) PEG (35 kDa) and 17% (v/v) Optiprep densifier; (2) shell solution with 4% (w/v) Hep-MA, 8%

(w/v) PEG4MAL (10 kDa), and 15 mM TEA; (3) shielding oil with mineral oil and 0.5% Span-80; (4) crosslinking emulsifier with 60 mM DTT dispersed in mineral oil with 3% Span-80. Each of the four solutions was filtered through 0.2 μm filters and loaded into syringes under sterile conditions and infused into separate inlets of a microfluidic device using syringe pumps (Harvard Apparatus) at the following rates: core (4 μL/min), shell (4 μL/min), shielding oil (50 μL/min), and crosslinking oil (60 μL/min). Microcapsules were then collected into 15 mL volume Falcon tube containing 1% BSA in 1× phosphate buffered saline (PBS) and incubated at 37 °C for 30 min. The capsules resided in the oil phase layer above the aqueous layer in the tube and slowly partitioned into the liquid phase. Mineral oil in the tube was aspirated, and microcapsules were harvested via a 100 μm cell strainer.

For the cell encapsulation experiments, H9 cells were digested by TrypLE^{TM} Express and re-suspended in the core solution at a concentration of 5×10^7 cells/mL. Flow rates of the core, shell, shielding oil, and crosslinker oil streams were maintained at 4, 4, 50, 60 μL/min, respectively. A cell suspension solution first was passed through the filter device and injected into the encapsulation device.[26] The H9 encapsulated microcapsules were collected into 15 mL tube filled with 5 mL mTeSR medium then distributed into a 6 well-plate and incubated at 37 °C with 5% CO_2.

2.5. Tannic acid-Fe^{3+} film (TA film) coating

2.5.1. TA film formation on planar substrates

We wanted to first use planar substrates to deposit and characterize TA films.[42, 43] Si wafers sputter-coated with 100 nm Au layer (10 mm by 10 mm) and SPR chips (Biosensing

Instruments) were cleaned by first immersing in isopropanol for 30 min while ultra-sonicating and then exposed to oxygen plasma for 3 min. Subsequently, the substrates were immersed in 1:2 mixture of Hep-thiol (0.5 mg/mL in 1× PBS) and PEG-thiol (1 mg/mL in 1× PBS) and kept overnight at 25°C in the dark. The substrates were rinsed three times with 1× PBS and dried using air. To deposit TA film, substrates containing a Hep-PEG layer were placed into 5 mL centrifuge tube, and 2.4 mL of DI water was added. Then, 0.3 mL of TA and $FeCl_3 \cdot 6H_2O$ solutions were sequentially added to adjust final concentrations of TA and $FeCl_3 \cdot 6H_2O$ in solution to 0.4 mg/mL and 0.1 mg/mL. To change pH to around 7, 1 M NaOH solution was added. The solution in the tube was vigorously agitated for 10 sec to form TA layer. Then, the gold substrate was washed with 1× PBS for 3 times to remove unbound TA and $FeCl_3 \cdot 6H_2O$. The film preparation process was repeated until desired number of layers was formed.

2.5.2. Coating on Hep microcapsules with TA film

The protocol for depositing TA film onto microcapsules was similar to coating of a planar substrate. Briefly 2,000 Hep microcapsules were placed in 2.4 mL of DI water in a 15 mL conical tube. Subsequently, 0.3 mL of TA (0.1 mg/mL) was added first, followed by 0.3 mL of $FeCl_3 \cdot 6H_2O$ (0.1 mg/mL). Immediately after color turned dark purple the reaction by mixing TA and Fe^{3+}, 4 μL of 1 M NaOH was added in order to reach to pH 7 to have tri-complexes of TA and Fe^{3+} in reaction.[42] This mixture was agitated by gentle pipetting for 10 sec. Then, the Hep microcapsules were collected using a 100 μm strainer to remove the residual solution and were washed with 1× PBS 5-7 times while on the strainer to remove unbound TA and $FeCl_3 \cdot 6H_2O$. The process was repeated in the exact same way to add new TA

layers.

2.5.3. Deposition TA film in monolayer cultures of hPSCs

We envisioned that TA deposits not only on the microcapsules but also on the encapsulated cells and wanted to assess whether such direct deposition of TA has positive or negative effects on viability and pluripotency of h9 cells. For this experiment, 1×10^5 cells/well of H9 cells were seeded on 6 well-plate and maintained in H9 pluripotency media for one day. Subsequently, media was aspirated, and cells were exposed to 0.1 mg/mL of TA and $FeCl_3 6H_2O$ in 1x PBS. Then, 1M of NaOH was added to adjust pH to neutral and the solution was agitated for 10 sec. The solution was removed and washed with 1× PBS5 times. The H9 cells were cultured in H9 media for 5 days and analyzed by RT-PCR for expression of pluripotency markers.

2.6. Characterization of TA coating

2.6.1. Thickness, surface topography, and amount measurement of TA film

Dried film thickness and surface topography of TA film on flat substrate was measured by ellipsometry (LSE-USB, Gaertner Scientific), and atomic force microscope (AFM; NX-10, Park Systems), respectively. For measurement of thickness changes (film degradation) under iron chelation conditions, Au thickness measurement of TA film degradation, the 3 layers of TA layers were prepared on Au-substrate. Then, the substrates were immersed into 1-50 mM of DFP aqueous solution at 37˚C for 3 days. At the certain time point, the film was dried, and its thickness was measured by ellipsometry.

The amount of TA deposited on a microcapsules was quantified using UV-vis spectroscopy (NanoDrop One-C; Thermofisher Scientific) as follows. Batches of 10,000 Hep capsules were coated with 1, 3 or 5 layers of TA as described before. Subsequently, capsules were immersed in 1 mM DFP solution at 37 ˚C for 3 days to degrade the TA film thoroughly (Figure S1). After complete degradation, the released TA in the solution could be detected by UV-vis absorption. The UV-vis absorption of DFP and TA was overlapped in the range of 200-300 nm wavelength (Figure S2). In order to minimize the DFP absorption effect, it was decided to consider only the 300 nm wavelength of the absorption range of TA. Absorbance of TA solution was then measured at 300 nm and the amount of TA was determined using a previously constructed calibration curve.

2.6.2. Surface plasmon resonance (SPR) analysis of bFGF binding to model surfaces

Au coated SPR chips were functionalized with Hep-PEG or Hep-PEG/TA film as described above in section 2.5.1. A solution of bFGF in 1× PBS (100 ng/mL, 120 μL) was injected over either Hep-PEG or Hep-PEG/TA surfaces at constant flow rate of 20 μL/min into the SPR device. SPR measurements were performed on Biosensing Instrument operated using Biosensing Instrument Control and Data analysis software (Biosensing Instrument Inc).

2.6.3. Microscopy characterization of TA film formation on microcapsules

TA layer adsorption onto microcapsules was characterized by fluorescence microscopy following a strategy described in the literature.[42] This strategy entailed labeling BSA with isothiocyanate in FITC using a standard protocol. Then, TA coated microcapsules were

incubated in 1 mg/mL of BSA-FITC in 1× PBS for 30 min at 37 ˚C. Similar protocol was used to visualize presence of TA film atop 2D cultures of H9 cells. After incubation with BSA-FITC and prior to fluorescence imaging capsules or cell cultures were washed 3 times with 1× PBS. Microscopy was carried out using standard fluorescence (IX83, Olympus) and confocal microscopes (LSM 780, ZEISS).

2.6.4. Assessing permeability of Hep microcapsule with and without TA film

To quantify permeability, 2,000 microcapsules were loaded with FITC-dextran (1 μM in 1× PBS, either 20 kDa, 70 kDa or 2,000 kDa) for 3 h at 37°C. Subsequently, microcapsules were quickly transferred into pristine 1× PBS solution and mounted onto a microscope (IX83, Olympus) to characterize release of fluorescent dextran. Images of microcapsules were analyzed using ImageJ. The same protocol was carried out for microcapsules carrying 0, 1 or 3 layers of TA.

2.6.5. Estimation of permeability and diffusivity of TA-coated microcapsules via MATLAB modeling

Diffusivity values were estimated using a custom-developed function in MATLAB (Mathworks, MA, USA). The function estimates permeability (m/s) of the dextran molecule across the microcapsule from the experimental intensity data normalized to initial (t=0) intensity. MATLAB function *pdepe* was used to solve the dimensionless form of unsteady diffusional transport equation and associated boundary and initial conditions:

$$\frac{\partial C'}{\partial t'} = \frac{1}{r'^2}\frac{\partial}{\partial r'}\left(r'^2\frac{\partial C'}{\partial r'}\right)$$

Initial Condition: $at\ t' = 0, C' = 1$

Boundary Conditions: $at\ r' = 0,\ \frac{\partial C'}{\partial r'} = 0, at\ r' = 1, \frac{\partial C'}{\partial r'} = -\alpha C'$

Here, $C' = \frac{C}{C_0}, r' = \frac{r}{R}, t' = \frac{tD}{R^2}, \alpha = \frac{PR}{D}$, R is the radius of the microcapsule (200 μm), C_0 is the initial intensity, D is the diffusivity of the dextran in the aqueous core (44 $\mu m^2/s$, 33 $\mu m^2/s$ and 0.9 $\mu m^2/s$ for 20, 70, and 2,000 kDa dextran respectively, Figure 2G), and P is the permeability of the dextran molecule in the shell. For an initial guess of the permeability value, the solution of the above equation yielded normalized concentration values as a function of the dimensionless radial position and at experimental time points. Concentration vs radial position data were integrated across the sphere and averaged to obtain mean intensity values vs time from the model. These were compared to experimental data at various time points and an objective function was established using summed square values of the error between the experimental data and model estimate. The objective function was minimized using the MATLAB function *fmincon* using α as a parameter to yield an optimal value of dextran permeability across the shell.

2.7. Loading and release of bFGF

We tested two different protocols for coating TA film and loading bFGF in Hep microcapsules. "coat-then-load" protocol involved depositing TA film first and loading bFGF second. This sequence was reversed for "load-then-coat" protocol (See the Figure 3A and 3B).

For “load-then-coat” protocol, 2,000 Hep microcapsules were placed into 2 mL of 100 ng/mL bFGF solution in 1× PBS for 3 h at 37˚C. Then, the microcapsules were collected using a 100 μm strainer and coated with either 1 or 3 layers of TA as described above. To establish a rigorous control for microcapsules without TA, we imitated the coating protocol (washing, pipetting etc.) but did not include TA-Fe reagents in solution. This condition, denoted Bare+Coating, was meant to account for loss of bFGF in the process of coating. “coat-then-load” protocol was carried out by first depositing 1 or 3 layers of TA onto microcapsules and then immersing microcapsules in bFGF solution as described above.

To assess release of bFGF, 2,000 microcapsules were placed on a 100 μm strainer inside 2 mL of 1× PBS in a well of a 6-well plate. Capsules were moved into fresh solution of 1× PBS at certain time points to collect residual solution. Concentration of bFGF remaining in solution was analyzed using ELISA according to the manufacturer’s protocol. The absorbance for bFGF amounts were measured by microplate reader (Synergy H1, BioTek; Winooski, VT, USA).

For bFGF-FITC loading and release test, synthesis of the FITC labeled bFGF was carried out following the previous studies.[44, 45] In order to bFGF-FITC loading and release of the Hep microcapsules, a similar experiment described above was performed. After bFGF-FITC loading, the Hep microcapsules were immediately moved to 1× PBS to let the conjugate be released out. The *in-situ* fluorescence intensity in Hep microcapsules was measured by fluorescence microscope.

2.8. Depositing TA film onto Hep microcapsules with stem cells and assessing pluripotency

After encapsulation, H9 cells were maintained in pluripotency media (mTeSR) for 1 day to promote spheroid formation. Then, Hep microcapsules were transferred into H9 media for 24 h to load bFGF. Deposition of TA layer was carried out as described above (section 2.5.2 TA film coating on Hep microcapsules). TA-coated or bare microcapsules were separated into two groups based on the mode of bFGF presentation and were cultured for additional 4 days. In one group, capsules were cultured in H9 media supplemented with bFGF. This group was called “soluble” throughout the paper. The other group of microcapsules was cultured in H9 media without bFGF. This group was called “immobilized” because encapsulated stem cells only experienced bFGF that was loaded at the beginning of the 5-day experiment. Same experimental groups were created for microcapsules that were first loaded with bFGF and then coated with TA.

2.9. Viability and proliferation of encapsulated H9 cells

H9 cell viability test was assessed using Live/Dead assay, where live and dead cells emitted green and red fluorescence, respectively. The Live/Dead staining was carried out following manufacturer’s protocol. Cells were imaged using fluorescence microscope and quantified with ImageJ software.

We used GFP-expressed H9 cells to quantify cell proliferation in microcapsules. Green fluorescence and brightfield images were acquired 1, 3, and 5 days after encapsulation. The spheroid size was assessed by ImageJ software.

2.10. Assessment of pluripotency with RT-PCR and immunofluorescence

To examine levels of pluripotency gene expression, 2,000 microcapsules were broken by applying electronic pestle for 5 min in cell lysis buffer, then total RNA was extracted using a commercial kit following manufacturer's instructions. Approximately 50-60 ng of total extracted RNA was used for synthesis of cDNA, following the reverse transcription kit protocol (Roche, Basel, Switzerland). The primer sequences used for RT-PCR are listed in Table S1. Gene expression was verified using QuantStudioTM 5 System (Thermofisher Scientific) with a SYBR Green and was normalized to the glyceraldehyde 3-phosphate dehydrogenase (GAPDH). The amplification procedure for Real-time PCR consists of 40 cycles of denaturation at 95℃ for 5 s, annealing at 55℃ for 15 s, and extension at 69℃ for 20 s. The final analysis was performed based on the threshold cycles using the ΔΔCT method.

For immunofluorescence staining, encapsulated or bare spheroids were fixed with 4% paraformaldehyde for 1 h and subsequently immersed in 30% v/v sucrose solution in 1× PBS for 24 h. Before cryo-sectioning, the spheroids were imbedded in OCT compound. The samples were sectioned into 10 μm thick slices using a cryostat (Leica CM1950; Buffalo Grove, IL, USA) and placed on a glass slide. The sectioned spheroids were then permeabilized by immersing in 0.1% Triton X-100 in 1× PBS solution for 20 min and blocked with 2% BSA-PBS for 1.5 h, at 25˚C. Then, the slides were incubated with primary Ab - 5 μg/mL of anti-Sox2 Abs in 1× PBS and 1% wt/v of BSA. Then, the slides were immersed in the solution of secondary Ab - 2 μg/mL of donkey anti-mouse IgG secondary antibody-Alexa Fluor 546 was treated for 1 h in the dark to conjugate to primary antibodies. Finally, 50 μL of mounting medium containing DAPI was dispensed onto sectioned spheroids and placed under a coverslip (170 μm; Fisher Healthcare). Imaging was imaged using an Olympus fluorescence microscope.

2.11. Statistical analysis

All experiments were performed at least in 3 replications. To verify the significance of each group in case of more than 3 groups, one-way ANOVA analysis followed by Tukey's post hoc was evaluated. For comparison significance of between 2 groups, paired Student's *t*-test for control and experimental data was evaluated. The significance was denoted as *, **, *** and NS, which means $p < 0.05$, $p < 0.01$, $p < 0.001$ and non-significant, respectively.

3. RESULTS AND DISCUSSION

3.1. Characterization of the TA film

Our team has an interest in developing microcapsules with PEG-Hep shell and an aqueous core that may be loaded with growth factors (GFs) for local and continuous delivery to the encapsulated stem cells.[26] In this paper, we wanted to test a hypothesis that coating a microcapsule with an ultrathin film may further enhance phenotype of the encapsulated stem cells by either slowing down the diffusion or improving the retention of GFs. To form an ultrathin coating, we focused on TA – a polyphenol with a glucose core – that has been shown to rapidly assemble into structured thin films in the presence of metal ions such as Fe^{3+}.[42, 43, 46] TA molecules interact with Fe ions via coordination bonding and form stable films of defined thickness. TA is a common food additive present in green tea or wine and, therefore, has excellent biocompatibility.[47, 48] We envisioned that a TA film will overcoat a microcapsule as shown in Figure 1A. However, before proceeding to microcapsule coating, we wanted to characterize properties of a TA film under better controlled conditions using surface analysis approaches. For this purpose, gold-coated Si substrates were functionalized using a 2:1 solution mixture of PEG-thiol and Hep-thiol in order to approximate the stoichiometry of PEG and Hep molecules in the hydrogel shell. The PEG-thiol and Hep-thiol molecules assembled and formed 2.5 nm layer on the substrate as measured by ellipsometry. A subsequent step of incubating a substrate in a solution containing TA and Fe^{3+} molecules resulted in deposition of a 6.5 nm layer (see Figure 1B). Interestingly, similar thickness increase was observed when depositing 2nd and 3rd layer of TA. Thus, ellipsometry analysis revealed that TA films formed on a substrate containing a Hep-PEG layer and that multiple TA layers could be assembled sequentially. Additional characterization of substrates was

performed by AFM. As shown in Figure 1C, deposition of TA film resulted in the appearance of sparsely dispersed 30 to 40 nm clusters. The presence of similar clusters has been reported previously and may represent non-uniformity in film formation or presence of TA-Fe^{3+} nucleation sites.[49-51] Deposition of 3 layers of TA film produced substrates with much denser distribution of the clusters. The surface roughness (Rq) increased from 4.108 nm to 6.682 nm for 1- and 3-layer TA film respectively. Thus, AFM analysis confirmed deposition of TA films onto PEG-Hep layer and pointed to expansion of nucleation sites as a growth mechanism.[52]

In the next set of experiments, we characterized deposition of TA film on Hep microcapsules. The microcapsules are fabricated using a flow focusing microfluidic device described in our previous publications and in Figure S3. Co-axial core and shell flow streams are ejected into the oil stream forming droplets. These droplets are then polymerized in situ, in the microfluidic device, by reaction of di-thiol cross-linker (DTT) with PEG4MAL molecules present in the shell. The core contains non-reactive high MW PEG molecules that leach out and are displaced by water molecules. The result is formation of microcapsules with a hydrogel shell (~10-15 μm) and an aqueous core.[26] These microcapsules were incubated in the solution containing TA and Fe^{3+} to create an ultrathin film. Because TA interacts with proteins via hydrogen bonding or hydrophobic interactions,[53] we used BSA-FITC to visualize presence of thin film. As seen from Figure 1D, BSA-FITC molecules interacted with TA-coated microcapsules but not with bare microcapsules. Confocal microscopy revealed that fluorescence signal localized to the perimeter of a capsule, forming ~2.84 μm and 6.81 μm annulus for 1-layer and 3-layer TA coating respectively. These observations pointed to penetration of TA molecules into and TA-Fe network growth inside the hydrogel – a behavior that was fundamentally different from planar substrates where TA film growth occurred

primarily in the xy plane.

As the next step, we quantified amount of TA deposited onto microcapsules as a function of layer number. To achieve this, coated microcapsules were incubated with an iron chelator DFP and then analyzed by spectrophotometry. TA concentrations were established using a calibration curve (see Figure S2). This experiment revealed that deposition of 1, 3 or 5 layers, resulted in 3.79 ng, 4.33 ng, and 5.31 ng of TA per capsule respectively. Unlike a solid substrate where the thickness (and the amount of deposited material) scaled linearly with the number of layers, the amount of TA adsorbed onto microcapsule increased only moderately and non-linearly with the number of layers. This may be explained by the different mode of film formation in the hydrogel that likely occurred along the polymeric segments and around water-retaining pores.

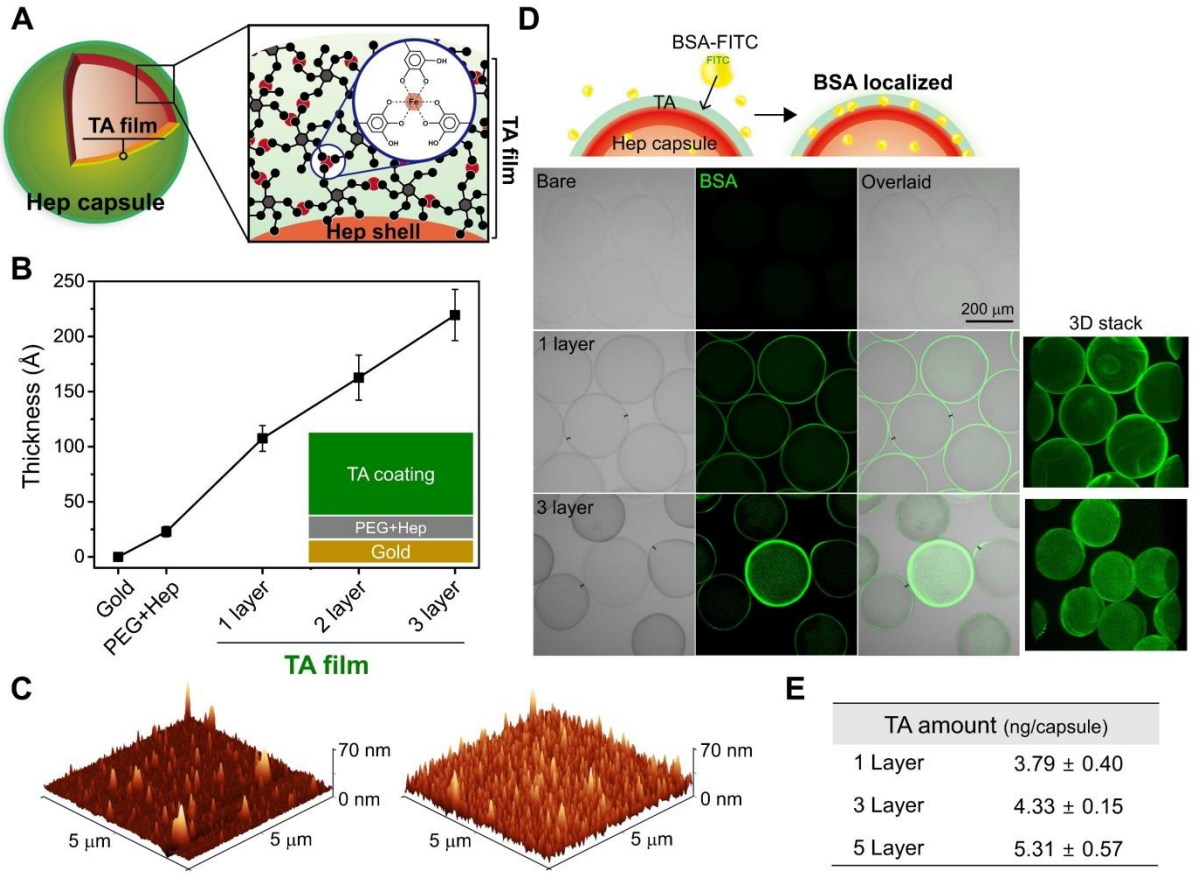

Figure 1. Characterization of TA film formation on model substrates and on microcapsules. (**A**) The chemistry of TA film with close-up view of the coordination complexes between TA and Fe ions. (**B**) Ellipsometry analysis of changes in thickness due to the deposition of multiple TA layers onto a model gold substrate containing PEG-SH/Hep-SH layer. (**C**) AFM analysis of topography for 1- and 3-layer TA coating. (**D**) Microcapsules coated with different number of TA layers were incubated in BSA-FITC and characterized by microscopy to visualize localization of TA film. (**E**) Microcapsules coated with TA layers were exposed to Fe chelator to disassemble the film. The amount of adsorbed TA was quantified using UV/Vis.

3.2. Assessing diffusivity of Hep microcapsules after deposition of TA film

Fluorescence imaging of FITC-dextran was used to assess diffusivity of microcapsules as a function of TA film deposition. In this experiment, microcapsules were first loaded by incubating with FITC-dextran (20, 70 or 2,000 kDa), and then transferred to pristine PBS solution to observe changes in fluorescence of microcapsules during release. In-capsule fluorescence was monitored and plotted over time to create release curves of the type shown in Figure 2 (A, C, and E). These data were also fitted to an unsteady-state diffusional transport equation to estimate diffusivity and permeability of the hydrogel shell for dextrans of different MWs.

The results of this experiment are compiled in Figure 2 and may be used to draw several observations. First, as shown in Figure 2A, the presence of one layer of TA resulted in modest (~1.4-fold) decrease in diffusivity for 20 kDa dextran when compared to bare capsules. 3-layer TA coating had 2.6-fold lower diffusivity compared to bare capsules. For both coating types, complete release occurred after 2 h (Figure 2B). Given that 20 kDa dextran approximates the size of bFGF, this observation suggests that TA coating was not expected to slow down diffusion of bFGF enough to affect a multi-day stem cell culture experiment.

In contrast, 70 kDa and 2,000 kDa dextrans diffused more slowly from overcoated microcapsules, with 40% to 60% of fluorescence retained in such microcapsules at a 30 min time point (Figure 2C-2F). Only 20-30% of fluorescence was observed in bare microcapsules at the same time point. It is also worth noting that residual in-capsule fluorescence was only observed at 2 h timepoint for 2000 kDa dextran release from microcapsules containing 3 layers of TA. This suggests once again that TA coating does not appreciably impede diffusion of large molecules. Given that hydrodynamic radii of 20, 70 and 2,000 kDa dextrans are ~4 nm, ~6 nm, and 27 nm, respectively,[54] we estimate the pore size for microcapsules without

TA coating and with 1 layer of TA film to be >30 nm. In the case of 3-layer TA coating pore size may be in the 10 to 25 nm range.

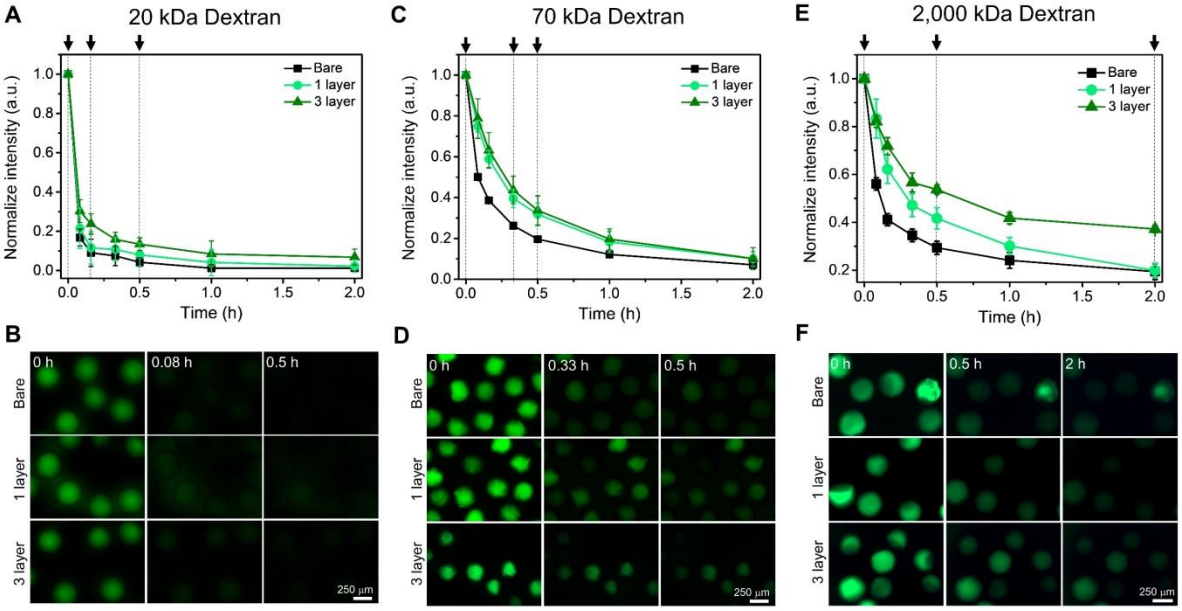

G

MW of dextran [kDa]	Diffusivity in Core [m²/s]	Type	Permeability [m/s]	Diffusivity in Shell [m²/s]
20	44×10^{-12}	Bare	7.94×10^{-7}	12.5×10^{-12}
		1 Layer	5.75×10^{-7}	9.07×10^{-12}
		3 Layer	3.01×10^{-7}	4.75×10^{-12}
70	33×10^{-12}	Bare	12.5×10^{-8}	19.8×10^{-13}
		1 Layer	5.38×10^{-8}	8.49×10^{-13}
		3 Layer	4.70×10^{-8}	7.41×10^{-13}
2,000	90×10^{-13}	Bare	19.9×10^{-8}	31.3×10^{-13}
		1 Layer	4.76×10^{-8}	7.51×10^{-13}
		3 Layer	2.23×10^{-8}	3.52×10^{-13}

Figure 2. Diffusivity of TA-coated microcapsules assessed using FITC-dextrans. Capsules were loaded with FITC-dextran and then moved to pristine solution to monitor decrease of in-capsule fluorescence over time. (**A**) In-capsule fluorescence as a function of TA layer number for diffusion of 20 kDa FITC-dextran. (**B**) Fluorescence images of microcapsules that correspond to black arrows in part A. (**C**) In-capsule fluorescence as a function of TA layer number for diffusion of 70 kDa FITC-dextran. (**D**) Fluorescence images of microcapsules that correspond to black arrows in part C. (**E**) In-capsule fluorescence analysis as a function of time for 2000 kDa FITC-dextran. (**F**) Fluorescence images that

correspond to time points identified with black arrows in part E. (**G**) Experimental results from parts A, C and E were fitted to a diffusion model in MATLAB to determine permeability and diffusivity values.

3.3. Effects of TA coating on loading and release of bFGF

Our goal is to use bioactive microcapsules for cultivation of pluripotent stem cells (PSCs). bFGF is the key inductive signal in most pluripotency maintenance protocols.[55] We have previously shown that Hep microcapsules retain and release bFGF in a controlled manner over the course of 5 days.[26] In this paper, we wanted to assess effects of TA film on release of bFGF from Hep microcapsules. We explored two modes of bFGF incorporation into overcoated microcapsules. 1) "load-then-coat" method, with microcapsules first incubated in 100 ng/mL bFGF solution for loading and then coated TA film. For this loading protocol, we had an additional experimental group called bare + coating that was designed to simulate rigorous washing involved in TA coating and to account for the potential loss of bFGF during such washing. We note that bFGF was loaded but the film was not deposited on capsules for bare + coating experimental group. 2) The other protocol explored here was "coat-then-load", with microcapsules first coated by TA and then loaded with bFGF.

Given that 1 and 3 layers were shown to result in the similar amount of TA incorporation into microcapsules as well as in similar diffusion properties for 20 and 70 kDa dextrans that best approximated size of GFs, henceforth, we focused on 1-layer TA coating. After loading bFGF, microcapsules were transferred into pristine PBS solution and maintained for 7-10 days with daily solution changes. ELISA was used to quantify 1) the amount of bFGF loaded after initial incubation and 2) release of bFGF over time. Figure 3 summarizes outcomes for this

set of experiments. Looking at the "load-then-coat" method for incorporating bFGF and TA into microcapsules (see Figure 3A-3C), it may be noted that the presence of TA coating resulted in much slower release of bFGF compared to bare microcapsules. At day 2, only 45% of bFGF was released from coated capsules compared to 80% from bare capsules. It is also worth noting that the amount of bFGF loaded into coated and bare microcapsules was similar, 19 and 17 ng respectively (per 2,000 capsules). The other scenario explored here was "coat-then-load" where TA film was first formed on microcapsules and bFGF was loaded as a second step. The experimental results for this scenario are described in Figure 3D-3F. It may be noted that differences in release profiles for this scenario were not as dramatic as those described for "load-then-coat" microcapsules. After 2 days, ~75% and 85% of bFGF was released from coated and bare microcapsules respectively. However, it was interesting to observe that the amount of loaded bFGF was 2-fold higher for coated microcapsules compared to bare microcapsules (~40 ng vs. ~21 ng per 2,000 capsules). This suggested that, in the coated microcapsules, Hep binding sites are supplemented with TA moieties resulting in greater capacity for uptake of bFGF.[56, 57] This observation is consistent with reports describing avid interactions of proteins with TA coatings via hydrogen bonding and hydrophobic interactions.[58, 59]

We went back to model substrates to carry out SPR analysis and confirm bFGF deposition onto chemical layers resembling those that comprised the microcapsules. This analysis (see Figure S4 and Table S2) revealed that deposition of TA layer atop Hep-PEG substrate resulted in ~3 fold higher adsorption of bFGF. SPR analysis on model substrates in combination with ELISA results for microcapsules confirm that presence of TA coating enhances loading of bFGF.

Our experiments underscore differences in loading and release of bFGF for the “load-then-coat” vs.“coat-then-load” modes of microcapsule preparation. For the former, the release appears to be slower likely because bFGF molecules imbedded in Hep hydrogel are diffusing through and bind to TA layer on the way out. For the latter mode of capsule preparation, bFGF molecules localize at TA/water interface and are released more rapidly, however, the loading capacity for bFGF is increased by a factor of 2. TA film may not represent an impediment to transport of bFGF but does dramatically increase loading capacity of microcapsules.

Taking dextran diffusion studies together with loading and release of bFGF, we conclude that TA coating does not appreciably affect diffusivity of a microcapsule but does enhance its capacity for binding bFGF. Thus, TA-GF affinity interactions governed slower release of bFGF from overcoated microcapsules observed in Figure 3 (A and C)

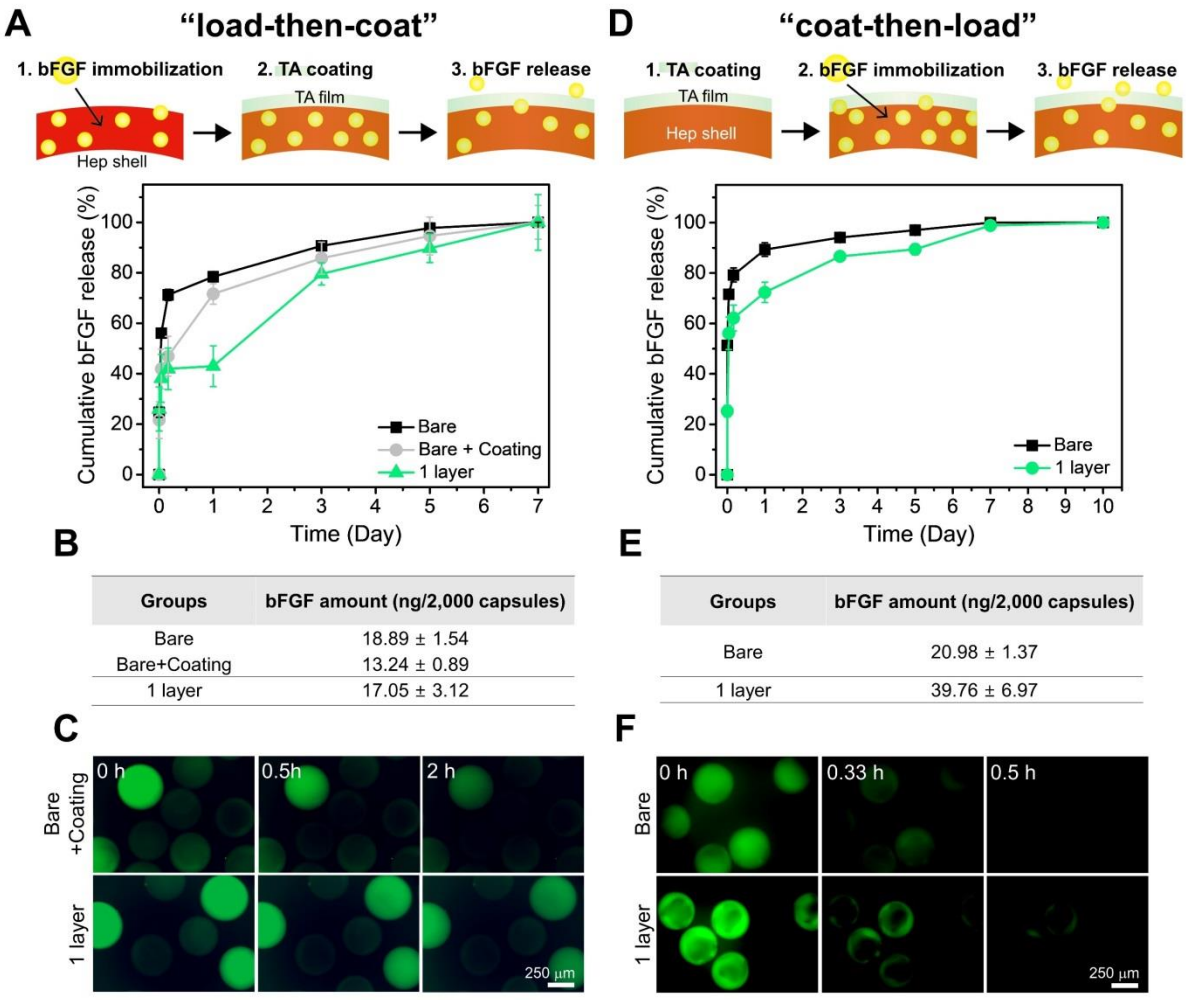

Groups	bFGF amount (ng/2,000 capsules)
Bare	18.89 ± 1.54
Bare+Coating	13.24 ± 0.89
1 layer	17.05 ± 3.12

Groups	bFGF amount (ng/2,000 capsules)
Bare	20.98 ± 1.37
1 layer	39.76 ± 6.97

Figure 3. Loading and release of bFGF from TA-coated microcapsules. (**A**) Microcapsules were first loaded with bFGF and then coated with TA film. Solution bathing microcapsules was sampled daily and analyzed by ELISA to establish cumulative release of bFGF. Microcapsules in bare + control group where exposed to rigorous washing associated with coating but did not receive TA coating. This was done to account for the possibility of GF release due to washing. (**B**) ELISA was used to determine the amount of bFGF loaded into microcapsules. (**C**) The use of FITC-labeled bFGF to confirm retention and release of this GF for "load-then-coat" microcapsules. (**D**) A different mode of ultrathin film assembly and GF loading where capsules were first overcoated with TA and then loaded with bFGF.

ELISA was used to determine bFGF release from microcapsules. (**E**) Results of ELISA analysis to of the bFGF loading into "coat-then-load" microcapsules. (**F**) Visualizing retention and release from "coat-then-load" microcapsules using FITC-labeled bFGF.

Description of experimental groups: *"load-then-coat"* – load bFGF and coat TA film on capsule; *Bare* – bare Hep microcapsules; *Bare + Coating* – Bare Hep microcapsules with only coating process in the absence of TA; *1 layer* – 1-layer TA-coated on bare Hep microcapsules. *"coat-then-load"* – coat TA layer first then load bFGF in capsules; *Bare* – bare Hep microcapsules; *1 layer* – 1-layer TA-coated on bare Hep microcapsules.

3.4. Assessing the effects of a TA coating on viability and proliferative capacity of the encapsulated pluripotent stem cells.

Having characterized effects of TA coating on loading and release of bFGF from microcapsules, we proceeded to investigate its effects on viability and proliferative capacity of hPSCs. Feeder-dependent H9 cells were used for these experiments. H9 cells were encapsulated with a flow focusing device described in Figure S3 using an input concentration of 50×10^6 cells/mL. A typical encapsulation run produced 400 μm diameter microcapsules with 90% cell occupancy,[25] 200 cells per capsule and viability > 90% (see Figures 4A, 4B and S5). Encapsulated H9 cells were placed into mTeSR media for 24 h and began to aggregate within that timeframe. TA coating was applied 1 day after encapsulation then microcapsules were switched to H9 pluripotency media (containing bFGF) and cultured for a total of 5 days. As seen from a panel of images in Figure 4C, spheroids proliferated rapidly inside microcapsules. Importantly, TA coating had no discernable effects on viability (Figure 4B) or proliferative capacity of H9 cells (Figure 4C and 4D). The results described in this section support the notion of TA coating being non-toxic to and compatible with the encapsulated hPSCs.

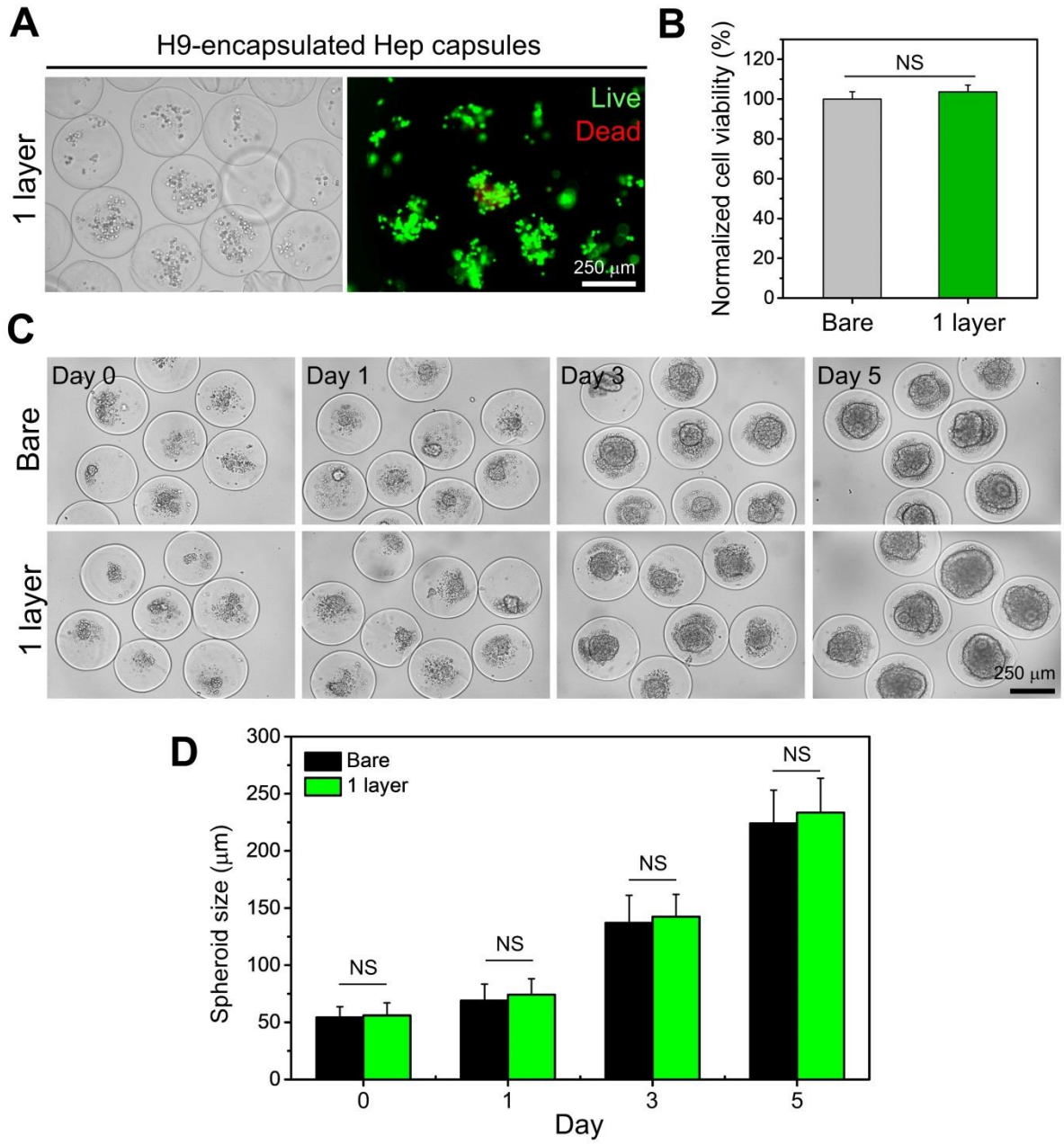

Figure 4. Assessing viability and proliferative capacity of encapsulated stem cells. (**A**) Brightfield and fluorescence (live/dead) images of H9 cells ~2h after encapsulation and TA coating. Cells were highly viable as indicated by green fluorescence and little to no red fluorescence. (**B**) Viability of cells in 10 capsules was analyzed using ImageJ. No significant differences in viability were observed between bare and TA-coated microcapsules. (**C**) Brightfield images recording stem cell spheroid size change in bare and coated microcapsules.

(D) Quantification of spheroid diameter change based on 25 microcapsules revealed no significant difference between bare and TA-coated microcapsules. (NS, $p > 0.05$).

3.5. Evaluating pluripotency of the encapsulated hPSCs

As the final step in our study, we wanted to evaluate how pluripotency maintenance of H9 cells is affected by encapsulation, TA coating and immobilization of bFGF. We have recently published a study that described encapsulation of feeder-independent HUES-8 cells that were adapted to 3D cultures.[25, 26] This past study demonstrated that Hep microcapsules loaded with bFGF and TGF-β1 supported pluripotent phenotype of HUES-8 cells. Importantly, inductive cues were loaded once and then were released locally to the encapsulated cells over the course of 5 days. The present study not only focuses on further enhancing bioactivity of microcapsules but also uses H9 cell line that is feeder dependent. We proceeded to characterize pluripotency of encapsulated stem cells, benchmarking it against standard cultures on feeders as well as against H9 spheroid cultures without capsules. Thus, we wanted to discern whether differences in pluripotency were due to bioactivity of microcapsule or the culture format (2D vs. 3D).

Is it possible that TA film deposits directly on the encapsulated stem cells and, if so, may it have a positive effect cell phenotype expression? To answer this question, we first investigated presence of TA moieties on the encapsulated cells. As before, BSA-FITC was employed for visualization of TA coating. As shown in Figure S6, we did indeed see co-localization of green fluorescence with encapsulated cells, suggesting that TA molecules deposited onto cells. As the next step we wanted to account for the possibility that TA had a direct positive effect on stem cell pluripotency, for example by binding and localizing bFGF

atop cells. We therefore created another control culture condition with H9 cells cultured on feeders and overcoated with TA film. This condition was denoted as 2D w/ TA.

As discussed in the preceding section, we studied two scenarios for loading microcapsules bFGF and coating with TA – "load-then-coat" and "coat-then-load". When compared with uncoated microcapsules, the former scenario was associated with slower release while the latter resulted in 2-fold higher incorporation of bFGF. Here we assessed pluripotency gene expression and carried out immunofluorescence staining for both types of microcapsules. In addition, we also compared the effects of one-time loading of bFGF into microcapsules and subsequent cultivation without bFGF in the media (denoted with superscript Imm), to exposure of encapsulated stem cells to soluble bFGF with daily media exchanges (denoted by superscript Sol).

Figure 5A summarizes RT-PCR analysis of three pluripotency genes for the "load-then-coat" microcapsules. First observation is that the three control groups without Hep gel (2D, 2D w/TA and spheroid) had similar levels of pluripotency gene expression after 5 days of culture in H9 pluripotency media complete with 100 ng/mL bFGF. This means that 1) TA coating deposited directly onto H9 cells did not improve their pluripotency and 2) 3D spheroid format alone did not contribute to improved pluripotency. Second observation was that H9 cells in bare Hep microcapsules (w/o TA coating) expressed significantly better levels of pluripotency genes compared to controls. The reader may remember that we wanted to account for potential loss of bFGF due to rigorous washing that is part of TA coating. Therefore, uncoated microcapsules were incubated with bFGF and then underwent a protocol that mimicked coating without depositing TA. This group was called Bare + coating (C). For this group, one-time loading of bFGF induced similar levels of Sox2 and Oct4 expression at day 5 of culture

compared to daily exposure to soluble bFGF during this timeframe. The exception was Nanog expression were Bare+C^{Sol} condition was significantly better than Bare+C^{Imm}. Third observation was that TA coating of microcapsules resulted in moderate but significant increase pluripotency gene expression compared to uncoated or bare microcapsules. Pluripotency was confirmed using immunofluorescence staining shown in Figure 5B and Figure S7.

Figure 5C summarizes pluripotency gene expression for "coat-then-load" microcapsules. Similar to the discussion above, H9 cells in Hep microcapsules expressed much better pluripotency compared to standard culture conditions (both 2D and 3D). Here, microcapsules coated with TA and exposed to soluble bFGF in pluripotency media (TA^{sol}) induced significantly better expression of pluripotent genes compared to uncoated microcapsules or to coated microcapsules loaded with bFGF without further supplementation of this signal in the media (TA^{Imm}). Significantly higher expression of Oct4 (3.94-fold) and Nanog (1.58-fold) was observed for "coat-then-load" compared to "load-then-coat" microcapsules compared to the $Bare^{Imm}$. Expression of Sox2 was not significantly different between the conditions. However, we should also note that immunofluorescence staining was used to confirm pluripotency expression in the encapsulated H9 cells (Figure 5D), resulting in more Sox2 expressed cells being indicated for TA^{Sol}.

The results described in Figure 5 are exciting for multiple reasons. First, we highlight that H9 cells cultured in bioactive microcapsules in the absence of feeder cells express pluripotency genes at a much higher level that in standard cultures on feeders. This suggests that higher level of pluripotency signaling in Hep microcapsules nullifies the need for feeders, at least for this particular cell line. We also highlight the fact that bioactive Hep-containing

microcapsules may be loaded with inductive cues for sustained release to the encapsulated stem cells. Such culture format may obviate the need for daily supplementation of soluble bFGF and may make cultivation of hPSC more affordable.

Finally, we demonstrate that presence of TA coating on Hep microcapsules further enhances their bioactivity. Here, coated microcapsules loaded with bFGF (immobilized condition), induced significantly better pluripotency gene expression compared bare microcapsules with either immobilized or soluble bFGF. We should note however that the best pluripotency gene expression was observed for "coat-then-load" microcapsules exposed to soluble bFGF. The reader may recall that such capsules had 2-fold better loading capacity for bFGF compared to standard Hep microcapsules. We therefore surmise that the ability to increase local concentration of bFGF afforded in these coated microcapsules translates into improved pluripotency.

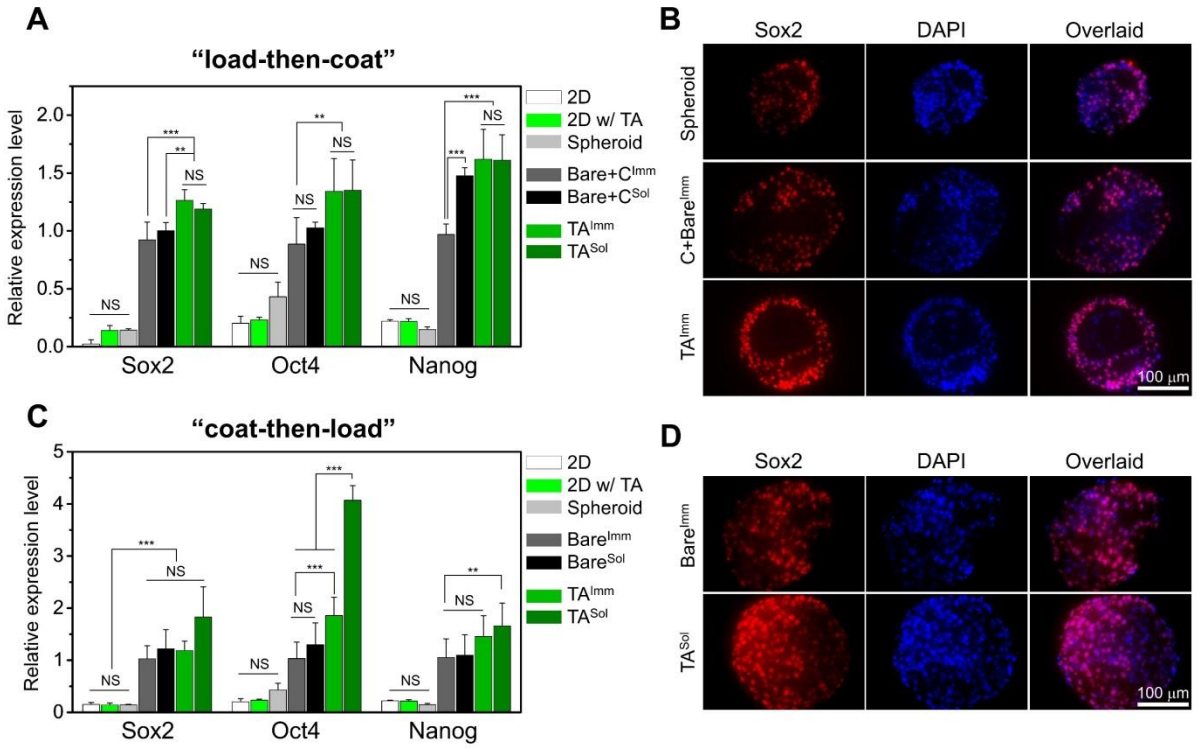

Figure 5. Analysis of pluripotency of the encapsulated stem cells. (**A**) RT-PCR analysis of pluripotency gene expression for stem cells in microcapsules prepared by "load-then-coat" method. Various experimental groups are described in greater detail below. (**B**) Immunofluorescence staining for Sox2 (red) and nuclei (blue, DAPI). (**C**) RT-PCR analysis of pluripotency gene expression for stem cells in microcapsules prepared by "coat-then-load" method. (D) Immunofluorescence staining for pluripotency marker Sox2 for stem cells in "coat-then-load" microcapsules. Statistical analysis – number of samples= 4 (ns, $p > 0.05$; *, $p \leq 0.05$; **, $p \leq 0.01$; ***, $p \leq 0.001$).

Description of experimental groups: *2D* – standard H9 cultures on MEF in pluripotency media; *2D w/TA* – as in previous but with TA coating, *spheroid* – H9 cell spheroids formed in 3D culture plates cultured in pluripotency media; *bare* + C^{Imm} - encapsulated H9 cells that exposed to rigorous washing without TA deposition; loaded with bFGF once and cultured without bFGF in the media; *Bare* + C^{Sol} – as in previous but bFGF was present in the media

during the experiment; TA^{Imm} – microcapsules loaded with bFGF, then overcoated with TA film and cultured without bFGF in the media; TA^{Sol} – as in previous but bFGF was present in the media throughout the experiment.

4. CONCLUSIONS

This study focused on ultrathin TA coating for modulating bioactivity of Hep-containing microcapsules. We first characterized TA film formation on model solid substrates and then explored coating of hydrogel microcapsules. This comparison revealed that while the amount of TA scaled linearly with the number of layers on a solid substrate, it increased only moderately on hydrogel microcapsules. We also noted that TA film/network formed not as an outer layer at the hydrogel shell-aqueous interface but within the hydrogel shell. While this remains to be proven experimentally, it is likely that TA deposition occurred along the polymer chains and around the water-filled pores of the hydrogel. TA coating was associated with only modest decrease in diffusivity across the hydrogel shell of microcapsules as confirmed with fluorescent dextrans. The TA coating did however have pronounced effects on increased loading and extended release of bFGF – an inductive cue commonly used for maintenance of pluripotent stem cells. Depending on the TA coating format, bFGF release could be extended from 5 to 7 days or its loading amount could be increased by a factor of 2 compared to uncoated Hep microcapsules. The improved loading and release characteristic of coated microcapsules are attributable to affinity interactions between TA moieties and bFGF molecules. Importantly, TA coating did not affect viability and proliferative capacity of pluripotent stem cells. In fact, TA-coated microcapsules induced better expression of pluripotency markers in the encapsulated H9 cells. To the best of our knowledge, this is the first description of an ultrathin coating used to improve bioactivity of microcapsules and maintenance of encapsulated pluripotent stem cells. Moving forward, we will leverage TA coated microcapsules to carry out stem cell differentiation studies along pancreatic and hepatic lineages. We also envision using the ability to assemble and disassemble TA coatings on demand to exercise more precise control over GF delivery to the encapsulated stem cells.

Acknowledgements

This study was supported in part by the grants from the Mayo Clinic Center for Regenerative Medicine, J.W. Kieckhefer Foundation, Al Nahyan Foundation, Regenerative Medicine Minnesota (RMM 101617 TR 004) and NIH (DK107255). Additional support was provided by an NIH Grant EB021911 to HB. Additional funding was provided by Mayo Clinic Center for Cell Signaling in Gastroenterology (P30DK084567).

References

1. Pera, M. F.; Reubinoff, B.; Trounson, A., Human embryonic stem cells. *Journal of cell science* **2000,** *113* (1), 5-10.

2. McDevitt, T. C.; Palecek, S. P., Innovation in the culture and derivation of pluripotent human stem cells. *Current opinion in biotechnology* **2008,** *19* (5), 527-533.

3. Gepstein, L., Derivation and potential applications of human embryonic stem cells. *Circulation research* **2002,** *91* (10), 866-876.

4. Stojkovic, M.; Lako, M.; Strachan, T.; Murdoch, A., Derivation, growth and applications of human embryonic stem cells. *Reproduction* **2004,** *128* (3), 259-267.

5. Martín, M.; Menéndez, P., Biological Impact of Human Embryonic Stem Cells. In *Stem Cell Transplantation*, Springer: 2012; pp 217-230.

6. Preynat-Seauve, O.; Suter, D. M.; Tirefort, D.; Turchi, L.; Virolle, T.; Chneiweiss, H.; Foti, M.; Lobrinus, J. A.; Stoppini, L.; Feki, A., Development of human nervous tissue upon differentiation of embryonic stem cells in three-dimensional culture. *Stem Cells* **2009,** *27* (3), 509-520.

7. Mohr, J. C.; de Pablo, J. J.; Palecek, S. P., 3-D microwell culture of human embryonic stem cells. *Biomaterials* **2006,** *27* (36), 6032-6042.

8. Lei, Y.; Jeong, D.; Xiao, J.; Schaffer, D. V., Developing defined and scalable 3D culture systems for culturing human pluripotent stem cells at high densities. *Cellular and molecular bioengineering* **2014,** *7* (2), 172-183.

9. Chaicharoenaudomrung, N.; Kunhorm, P.; Noisa, P., Three-dimensional cell culture systems as an in vitro platform for cancer and stem cell modeling. *World journal of stem cells* **2019,** *11* (12), 1065.

10. Cerdan, C.; Hong, S. H.; Bhatia, M., Formation and hematopoietic differentiation of

human embryoid bodies by suspension and hanging drop cultures. *Current protocols in stem cell biology* **2007,** *3* (1), 1D. 2.1-1D. 2.16.

11. Yoon, B. S.; Yoo, S. J.; Lee, J. E.; You, S.; Lee, H. T.; Yoon, H. S., Enhanced differentiation of human embryonic stem cells into cardiomyocytes by combining hanging drop culture and 5-azacytidine treatment. *Differentiation* **2006,** *74* (4), 149-159.

12. Smith, L. A.; Liu, X.; Hu, J.; Ma, P. X., The enhancement of human embryonic stem cell osteogenic differentiation with nano-fibrous scaffolding. *Biomaterials* **2010,** *31* (21), 5526-5535.

13. Rohani, L.; Borys, B. S.; Razian, G.; Naghsh, P.; Liu, S.; Johnson, A. A.; Machiraju, P.; Holland, H.; Lewis, I. A.; Groves, R. A., Stirred suspension bioreactors maintain naïve pluripotency of human pluripotent stem cells. *Communications biology* **2020,** *3* (1), 1-22.

14. Lam, A. T.-L.; Li, J.; Toh, J. P.-W.; Sim, E. J.-H.; Chen, A. K.-L.; Chan, J. K.-Y.; Choolani, M.; Reuveny, S.; Birch, W. R.; Oh, S. K.-W., Biodegradable poly-ε-caprolactone microcarriers for efficient production of human mesenchymal stromal cells and secreted cytokines in batch and fed-batch bioreactors. *Cytotherapy* **2017,** *19* (3), 419-432.

15. Ting, S.; Chen, A.; Reuveny, S.; Oh, S., An intermittent rocking platform for integrated expansion and differentiation of human pluripotent stem cells to cardiomyocytes in suspended microcarrier cultures. *Stem cell research* **2014,** *13* (2), 202-213.

16. Borys, B. S.; So, T.; Colter, J.; Dang, T.; Roberts, E. L.; Revay, T.; Larijani, L.; Krawetz, R.; Lewis, I.; Argiropoulos, B., Optimized serial expansion of human induced pluripotent stem cells using low-density inoculation to generate clinically relevant quantities in vertical-wheel bioreactors. *Stem cells translational medicine* **2020,** *9* (9), 1036-1052.

17. Zhao, S.; Xu, Z.; Wang, H.; Reese, B. E.; Gushchina, L. V.; Jiang, M.; Agarwal, P.; Xu, J.; Zhang, M.; Shen, R., Bioengineering of injectable encapsulated aggregates of

pluripotent stem cells for therapy of myocardial infarction. *Nature communications* **2016,** *7* (1), 1-12.

18. Zhang, W.; Zhao, S.; Rao, W.; Snyder, J.; Choi, J. K.; Wang, J.; Khan, I. A.; Saleh, N. B.; Mohler, P. J.; Yu, J., A novel core–shell microcapsule for encapsulation and 3D culture of embryonic stem cells. *Journal of materials chemistry B* **2013,** *1* (7), 1002-1009.

19. Choe, G.; Kim, S.-W.; Park, J.; Park, J.; Kim, S.; Kim, Y. S.; Ahn, Y.; Jung, D.-W.; Williams, D. R.; Lee, J. Y., Anti-oxidant activity reinforced reduced graphene oxide/alginate microgels: mesenchymal stem cell encapsulation and regeneration of infarcted hearts. *Biomaterials* **2019,** *225*, 119513.

20. Siti-Ismail, N.; Bishop, A. E.; Polak, J. M.; Mantalaris, A., The benefit of human embryonic stem cell encapsulation for prolonged feeder-free maintenance. *Biomaterials* **2008,** *29* (29), 3946-3952.

21. Serra, M.; Correia, C.; Malpique, R.; Brito, C.; Jensen, J.; Bjorquist, P.; Carrondo, M. J.; Alves, P. M., Microencapsulation technology: a powerful tool for integrating expansion and cryopreservation of human embryonic stem cells. *PloS one* **2011,** *6* (8), e23212.

22. Choe, G.; Park, J.; Park, H.; Lee, J. Y., Hydrogel biomaterials for stem cell microencapsulation. *Polymers* **2018,** *10* (9), 997.

23. Xu, J.; Shamul, J. G.; Staten, N. A.; White, A. M.; Jiang, B.; He, X., Bioinspired 3D Culture in Nanoliter Hyaluronic Acid-Rich Core-Shell Hydrogel Microcapsules Isolates Highly Pluripotent Human iPSCs. *Small* **2021,** *17* (33), 2102219.

24. Finklea, F. B.; Tian, Y.; Kerscher, P.; Seeto, W. J.; Ellis, M. E.; Lipke, E. A., Engineered cardiac tissue microsphere production through direct differentiation of hydrogel-encapsulated human pluripotent stem cells. *Biomaterials* **2021,** *274*, 120818.

25. Fattahi, P.; Rahimian, A.; Slama, M. Q.; Gwon, K.; Gonzalez-Suarez, A. M.; Wolf, J.;

Baskaran, H.; Duffy, C. D.; Stybayeva, G.; Peterson, Q. P., Core–shell hydrogel microcapsules enable formation of human pluripotent stem cell spheroids and their cultivation in a stirred bioreactor. *Scientific reports* **2021,** *11* (1), 1-13.

26. Gwon, K.; Hong, H. J.; Gonzalez-Suarez, A. M.; Slama, M. Q.; Choi, D.; Hong, J.; Baskaran, H.; Stybayeva, G.; Peterson, Q. P.; Revzin, A., Bioactive hydrogel microcapsules for guiding stem cell fate decisions by release and reloading of growth factors. *Bioactive Materials* **2021**.

27. Macdonald, M. L.; Samuel, R. E.; Shah, N. J.; Padera, R. F.; Beben, Y. M.; Hammond, P. T., Tissue integration of growth factor-eluting layer-by-layer polyelectrolyte multilayer coated implants. *Biomaterials* **2011,** *32* (5), 1446-1453.

28. Min, J.; Braatz, R. D.; Hammond, P. T., Tunable staged release of therapeutics from layer-by-layer coatings with clay interlayer barrier. *Biomaterials* **2014,** *35* (8), 2507-2517.

29. Damanik, F. F.; Brunelli, M.; Pastorino, L.; Ruggiero, C.; Van Blitterswijk, C.; Rotmans, J.; Moroni, L., Sustained delivery of growth factors with high loading efficiency in a layer by layer assembly. *Biomaterials Science* **2020,** *8* (1), 174-188.

30. Han, U.; Kim, Y. J.; Kim, W.; Park, J. H.; Hong, J., Construction of nano-scale cellular environments by coating a multilayer nanofilm on the surface of human induced pluripotent stem cells. *Nanoscale* **2019,** *11* (28), 13541-13551.

31. Han, U.; Kim, W.; Cha, H.; Park, J. H.; Hong, J., Nano-structure of vitronectin/heparin on cell membrane for stimulating single cell in iPSC-derived embryoid body. *Iscience* **2021,** *24* (4), 102297.

32. Abouelmagd, S. A.; Abd Ellah, N. H.; Amen, O.; Abdelmoez, A.; Mohamed, N. G., Self-assembled tannic acid complexes for pH-responsive delivery of antibiotics: Role of drug-carrier interactions. *International Journal of Pharmaceutics* **2019,** *562*, 76-85.

33. Mori, T.; Rezai-Zadeh, K.; Koyama, N.; Arendash, G. W.; Yamaguchi, H.; Kakuda, N.; Horikoshi-Sakuraba, Y.; Tan, J.; Town, T., Tannic acid is a natural β-secretase inhibitor that prevents cognitive impairment and mitigates Alzheimer-like pathology in transgenic mice. *Journal of Biological chemistry* **2012,** *287* (9), 6912-6927.

34. Shutava, T.; Prouty, M.; Kommireddy, D.; Lvov, Y., pH responsive decomposable layer-by-layer nanofilms and capsules on the basis of tannic acid. *Macromolecules* **2005,** *38* (7), 2850-2858.

35. Zhang, W.; Besford, Q. A.; Christofferson, A. J.; Charchar, P.; Richardson, J. J.; Elbourne, A.; Kempe, K.; Hagemeyer, C. E.; Field, M. R.; McConville, C. F., Cobalt-directed assembly of antibodies onto metal–phenolic networks for enhanced particle targeting. *Nano Letters* **2020,** *20* (4), 2660-2666.

36. Guo, Z.; Xie, W.; Lu, J.; Guo, X.; Xu, J.; Xu, W.; Chi, Y.; Takuya, N.; Wu, H.; Zhao, L., Tannic acid-based metal phenolic networks for bio-applications: a review. *Journal of Materials Chemistry B* **2021,** *9* (20), 4098-4110.

37. Hagerman, A. E., Chemistry of tannin-protein complexation. In *Chemistry and significance of condensed tannins*, Springer: 1989; pp 323-333.

38. Lee, H.; Dellatore, S. M.; Miller, W. M.; Messersmith, P. B., Mussel-inspired surface chemistry for multifunctional coatings. *science* **2007,** *318* (5849), 426-430.

39. Tae, G.; Kim, Y.-J.; Choi, W.-I.; Kim, M.; Stayton, P. S.; Hoffman, A. S., Formation of a novel heparin-based hydrogel in the presence of heparin-binding biomolecules. *Biomacromolecules* **2007,** *8* (6), 1979-1986.

40. Gwon, K.; Kim, E.; Tae, G., Heparin-hyaluronic acid hydrogel in support of cellular activities of 3D encapsulated adipose derived stem cells. *Acta biomaterialia* **2017,** *49*, 284-295.

41. Gwon, K.; Hong, H. J.; Gonzalez-Suarez, A. M.; Stybayeva, G.; Revzin, A., Microfluidic Fabrication of Core-Shell Microcapsules carrying Human Pluripotent Stem Cell Spheroids. *Journal of Visualized Experiments: Jove* **2021,** (176).

42. Ejima, H.; Richardson, J. J.; Liang, K.; Best, J. P.; van Koeverden, M. P.; Such, G. K.; Cui, J.; Caruso, F., One-step assembly of coordination complexes for versatile film and particle engineering. *Science* **2013,** *341* (6142), 154-157.

43. Lee, J.; Cho, H.; Choi, J.; Kim, D.; Hong, D.; Park, J. H.; Yang, S. H.; Choi, I. S., Chemical sporulation and germination: cytoprotective nanocoating of individual mammalian cells with a degradable tannic acid–Fe III complex. *Nanoscale* **2015,** *7* (45), 18918-18922.

44. Wu, J.; Liu, Y.; Cao, Q.; Yu, T.; Zhang, J.; Liu, Q.; Yang, X., Growth factors enhanced angiogenesis and osteogenesis on polydopamine coated titanium surface for bone regeneration. *Materials & Design* **2020,** *196*, 109162.

45. Choi, G. H.; Lee, H. J.; Lee, S. C., Titanium-A dhesive Polymer Nanoparticles as a Surface-R eleasing System of Dual Osteogenic Growth Factors. *Macromolecular bioscience* **2014,** *14* (4), 496-507.

46. Yun, G.; Richardson, J. J.; Capelli, M.; Hu, Y.; Besford, Q. A.; Weiss, A. C.; Lee, H.; Choi, I. S.; Gibson, B. C.; Reineck, P., The biomolecular corona in 2D and reverse: patterning metal–phenolic networks on proteins, lipids, nucleic acids, polysaccharides, and fingerprints. *Advanced Functional Materials* **2020,** *30* (1), 1905805.

47. Turgut Coşan, D.; Saydam, F.; Özbayer, C.; Doğaner, F.; Soyocak, A.; Güneş, H. V.; Değirmenci, İ.; Kurt, H.; Üstüner, M. C.; Bal, C., Impact of tannic acid on blood pressure, oxidative stress and urinary parameters in L-NNA-induced hypertensive rats. *Cytotechnology* **2015,** *67* (1), 97-105.

48. Wang, Y.; Liu, S.; Ding, K.; Zhang, Y.; Ding, X.; Mi, J., Quaternary tannic acid with

improved leachability and biocompatibility for antibacterial medical thermoplastic polyurethane catheters. *Journal of Materials Chemistry B* **2021,** *9* (23), 4746-4762.

49. Huang, Y.; Lin, Q.; Yu, Y.; Yu, W., Functionalization of wood fibers based on immobilization of tannic acid and in situ complexation of Fe (II) ions. *Applied Surface Science* **2020,** *510*, 145436.

50. Li, D.; Shen, H.; Cai, C.; Sun, T.; Zhao, Y.; Chen, L.; Zhao, N.; Xu, J., Fabrication of conductive silver microtubes using natural catkin as a template. *ACS omega* **2017,** *2* (4), 1738-1745.

51. Rahim, M. A.; Ejima, H.; Cho, K. L.; Kempe, K.; Müllner, M.; Best, J. P.; Caruso, F., Coordination-driven multistep assembly of metal–polyphenol films and capsules. *Chemistry of Materials* **2014,** *26* (4), 1645-1653.

52. Lee, H.; Nguyen, D. T.; Kim, N.; Han, S. Y.; Hong, Y. J.; Yun, G.; Kim, B. J.; Choi, I. S., Enzyme-Mediated Kinetic Control of Fe3+–Tannic Acid Complexation for Interface Engineering. *ACS Applied Materials & Interfaces* **2021,** *13* (44), 52385-52394.

53. Choi, D.; Heo, J.; Hong, J., Controllable drug release from nano-layered hollow carrier by non-human enzyme. *Nanoscale* **2018,** *10* (38), 18228-18237.

54. Pilz, M.; Kwapiszewska, K.; Kalwarczyk, T.; Bubak, G.; Nowis, D.; Hołyst, R., Transport of nanoprobes in multicellular spheroids. *Nanoscale* **2020,** *12* (38), 19880-19887.

55. Mossahebi-Mohammadi, M.; Quan, M.; Zhang, J.-S.; Li, X., FGF signaling pathway: a key regulator of stem cell pluripotency. *Frontiers in Cell and Developmental Biology* **2020,** *8*, 79.

56. Choi, D.; Komeda, M.; Heo, J.; Hong, J.; Matsusaki, M.; Akashi, M., Vascular endothelial growth factor incorporated multilayer film induces preangiogenesis in endothelial cells. *ACS Biomaterials Science & Engineering* **2018,** *4* (5), 1833-1842.

57. Shin, M.; Lee, H.; Lee, M.; Shin, Y.; Song, J.-J.; Kang, S.-W.; Nam, D.-H.; Jeon, E. J.; Cho, M.; Do, M., Targeting protein and peptide therapeutics to the heart via tannic acid modification. *Nature biomedical engineering* **2018,** *2* (5), 304-317.

58. Van Buren, J. P.; Robinson, W. B., Formation of complexes between protein and tannic acid. *Journal of Agricultural and Food Chemistry* **1969,** *17* (4), 772-777.

59. Siebert, K. J.; Troukhanova, N. V.; Lynn, P. Y., Nature of polyphenol− protein interactions. *Journal of Agricultural and Food Chemistry* **1996,** *44* (1), 80-85.